Electronic Supplementary Material (ESI) for Nanoscale.

Supporting Information

Accelerated Crystallization and Encapsulation for Synthesis of Water- and Oxygen-Resistant Perovskite Nanoparticles in Microdroplets

*Zi Long, Yan Wang, Qiang Fu, Jin Ouyang, Lixin He and Na Na**

Key Laboratory of Theoretical and Computational Photochemistry, College of Chemistry, Beijing Normal University, Beijing 100875, China.

Experimental Section

Chemical reagents. The following reagents were used: hydrobromic acid (pure, ca. 48 wt% solution in water, Acros), methylamine pure (2 M solution in methanol, Acros), lead(II) bromide ($PbBr_2$, Puratronic, 99.999%, Alfa Aesar), polycarbonate resin (PC, approx. M.W. 45,000, pellets, Acros), cellulose acetate (CA, Aldrich, approx. M.W. 50,000), poly(styrene) (PS, average M.W. 250,000, Acros), poly(methyl methacrylate) (PMMA, beads, average M.W. 35,000, Acros), poly(vinylpyrrolidone) (PVP, M.W. 58,000), N,N-dimethylformamide (DMF, 99.9%, extra dry, Innochem.), fetal bovine serum (FBS) and Dulbecco's Modified Eagle's Medium (DMEM, Invitrogen, Thermo Fisher Scientific, USA), phosphate buffered saline (PBS, 0.01 M, pH =7.2-7.4, Solarbio, Beijing Solarbio Science & Technology Co., Ltd.), and 4',6-diamidino-2-phenylindole (DAPI, 2 μg/mL, Sigma-Aldrich). Amino acids and metal salts were obtained from Sinopharm Chemical Reagent Beijing Co., Ltd. Female BALB/c nude mice (6-7 weeks, 18-22 g) were used for Fe^{3+} and $_L$-Cys detection and were purchased from Beijing Vital River Laboratories (China). All chemicals were of analytical grade or better and used without further purification. Deionized water (Mill-Q, Millipore, 18.2 MΩ) was used in all experiments. CH_3NH_3Br (MABr) was synthesized following the reported method.[1]

Apparatus and Software. Transmission electron microscopy (TEM) imaging was performed on a FEI Talos 200s transmission electron microscope with an operating voltage of 200 kV. Field emission scanning electron microscopy (FESEM, S-8010, Hitachi). UV2600 spectrophotometer (Shimadzu, Japan). FLS980 fluorescence spectrophotometer (Edinburgh Instruments, UK). X-ray diffraction measurements were performed with a Maxima XRD-7000 (Shimadzu, Japan). Dynamic light scattering (DLS) was carried out on a Nano-ZS Zetasizer ZEN3600 (Malvern Instruments Ltd., U.K.). The in vitro cytotoxicity assay was measured at 490 nm in a microplate reader (BioTek Instruments Inc., USA). Confocal laser scanning microscopy (CLSM) was operated on a Nikon A1R. In vivo imaging was carried out on an IVIS Lumina III system (Caliper, USA). The rate of droplet formation at the needle tip was controlled by a peristaltic pump from Longer Precision Pump Co., Ltd. (LSP01-1A), the high voltage was supplied by a DC high-voltage power supply (China, HB-Z303-1AC). A Nikon stereoscopic microscope (SMZ18), Nikon D5 camera and red-ray laser (100 mW, 650 nm) were used for video recording of the spray formation. The speed of the particles was measured by particle image velocimetry (PIV, Dantec), and particles were illuminated by a double-pulsed Nd:YAG 532 nm laser (ZK-Laser Beijing Co., LTD). A high-speed optical camera (Phantom 9060; Vision Research) was used to image the generation, fusion, and trajectories of the droplets. The data obtained from PIV were processed by Tecplot 360 EX 2017 R2 software to calculate the average speed of the particles.

Average Droplet Speed Measurement by Particle Imaging Velocimetry. By means of PIV, the average speeds of the droplets were measured. Particles were illuminated by a double-pulsed Nd:YAG 532 nm laser with a double cavity. The dimensions of the interrogation were 32×32 pixels. The time between pulses was set to 70 μs. A high-speed CMOS optical camera (Phantom 9060; Vision Research) of 1280 pixels×800 pixels with a spatial resolution of 128.0 mm×102.4 mm was used to acquire images of the generation, fusion, and trajectories of the droplets. The distance between the needle tip and laser was approximately 0.8 m. The synchronization between laser and camera was made by means of a synchronizer BNC 575. A total of 2000 image pairs were recorded for one second, and each measurement in our work lasted three seconds.

In Vitro Cytotoxicity Assay. To examine the cell toxicity, the standard 3-(4,5-dimethylthiazol-2-yl)-2,5-diphenyltetrazolium bromide (MTT) assay was applied to assess the toxicity of the PC-PNPs using HepG2 cells. The cells were incubated at 37 °C in DMEM containing 10% FBS under an atmosphere of 5% CO_2 for 24 h. Then, the PC-PNPs with different concentrations were added into the different wells to incubate with the HepG2 cells for 24 h (5 parallel experiments were performed for every concentration of NPs). Whereafter, 20 μL of a 5 mg/mL MTT solution in PBS (pH = 7.2-7.4) was added into each well and further incubated for 4 hours. The supernatant in each well was removed, and 150 μL of dimethylsulfoxide (DMSO) was added to each well to dissolve the MTT formazan crystals. Then, the absorbance was recorded at 490 nm in a microplate reader. Cell viability was calculated as the percentage of viable cells after being treated with NPs compared with the number of untreated cells.

Cellular Fluorescence Imaging. The digested HepG2 cells were placed into confocal Petri dishes in 1.5 mL of DMEM with 10% FBS and incubated for 12 h (at 37 °C in 5% CO_2). The prepared PC-PNPs were added into the above dishes and incubated in 5% CO_2 at 37 °C for different time (0, 4, 12 and 20 h). Then, the medium was discarded, and the cells were washed with PBS (pH = 7.2-7.4) three times, fixed by cold methanol (1 mL) at -20 °C in a refrigerator for approximately 12 min, and then rinsed with PBS three times. Thereafter, DAPI (2 μg/mL in PBS) was applied to stain the cell nuclei for approximately 10 min at 37 °C away from light and then washed with PBS three times. Then, the images of the HepG2 cells were recorded by CLSM.

In Vivo Detection. Female BALB/c nude mice (aged 6-7 weeks, 18-22 g) were used for in vivo imaging. All mice were anesthetized by isoflurane before subcutaneous injection and the subsequent imaging. The reagents were injected into the left thigh of the mice, and the imaging was employed 5 min later. The excitation wavelength was 420 nm, and the emission wavelength was 520 nm. All experiments requiring the use of mice were authorized by the animal care committee of Beijing Normal University.

Supplementary Results

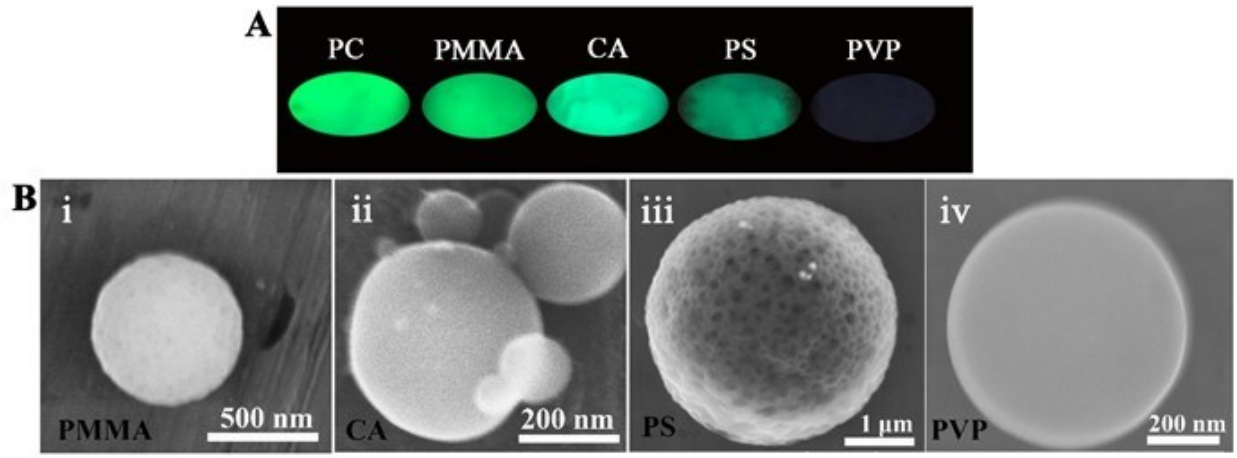

Fig. S1 Optimization of the polymer. (A) FL photographs of the different polymer-PNPs collected on the receptor in solid phase. Excitation wavelength: 365 nm. (B) SEM images of the different polymer-PNPs (PMMA, CA, PS and PVP).

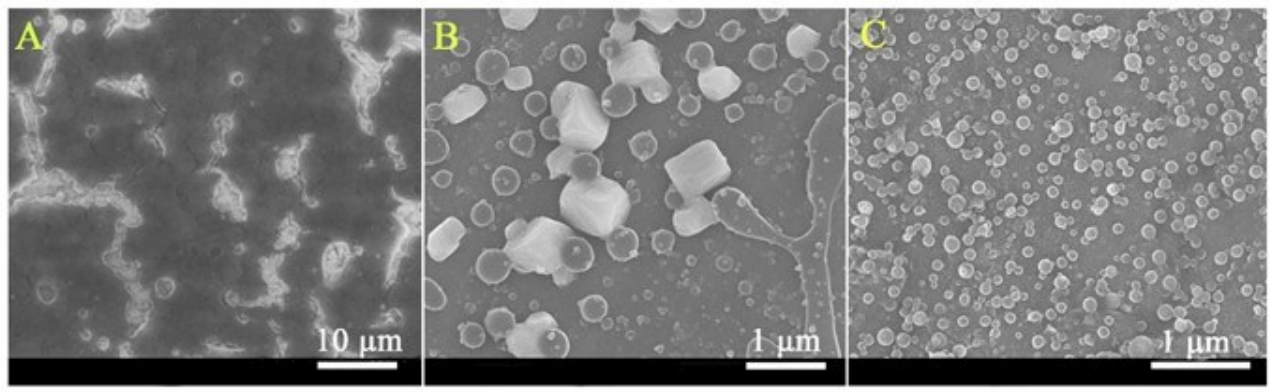

Fig. S2 SEM images of the PC-encapsulated perovskite NPs synthesized under different spray voltages (A) 8 kV, (B) 14 kV, and (C) 20 kV.

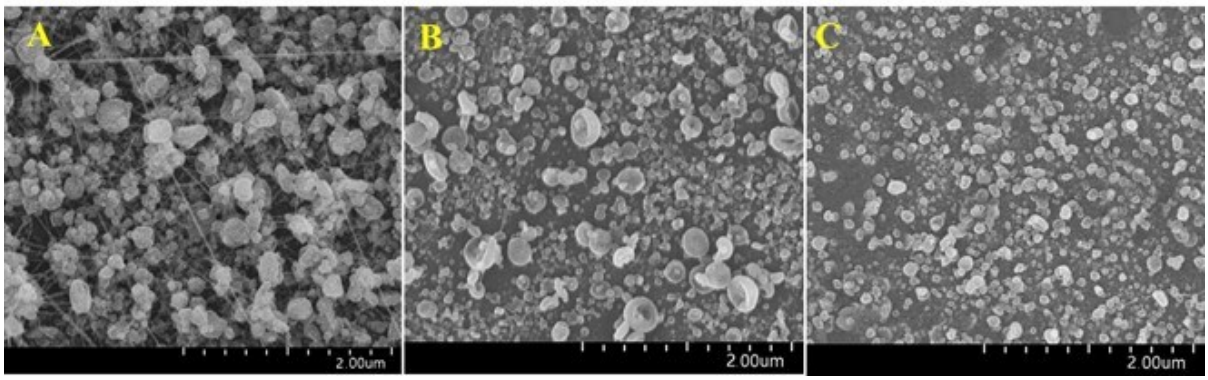

Fig. S3 SEM images of the PC-PNPs synthesized with different spray times. (A) 24 ms, (B) 40 ms, and (C) 100 ms.

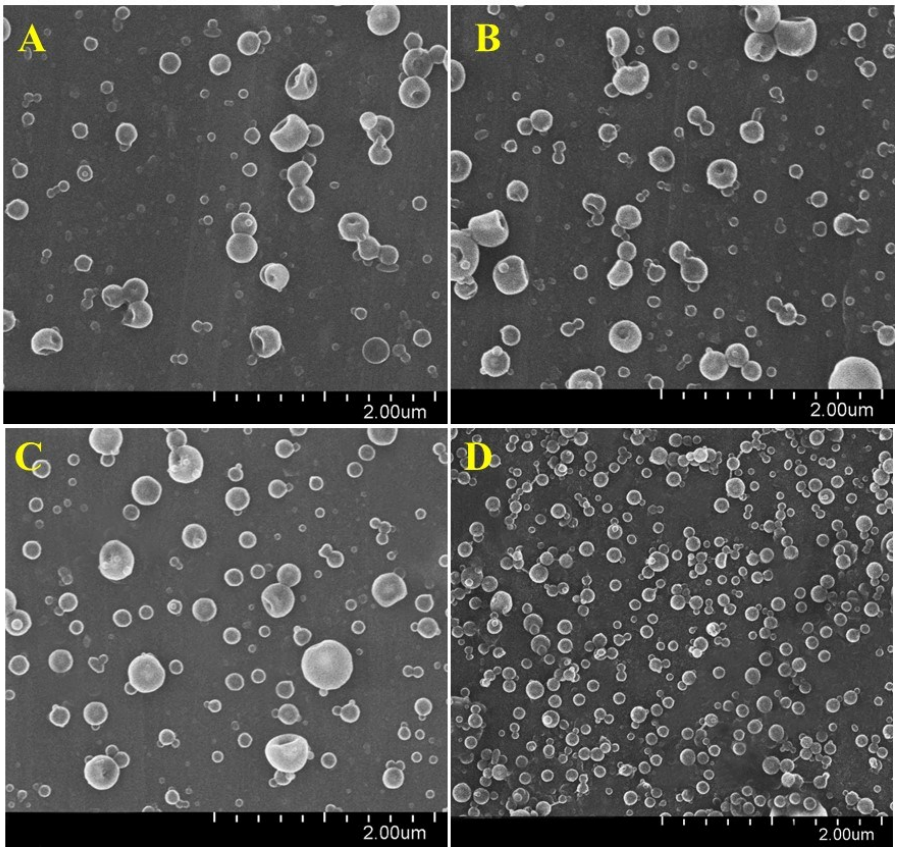

Fig. S4 SEM images of the PC-PNPs synthesized with different flow rates, (A) 3 μL/min, (B) 2 μL/min, (C) 1 μL/min, and (D) 0.5 μL/min.

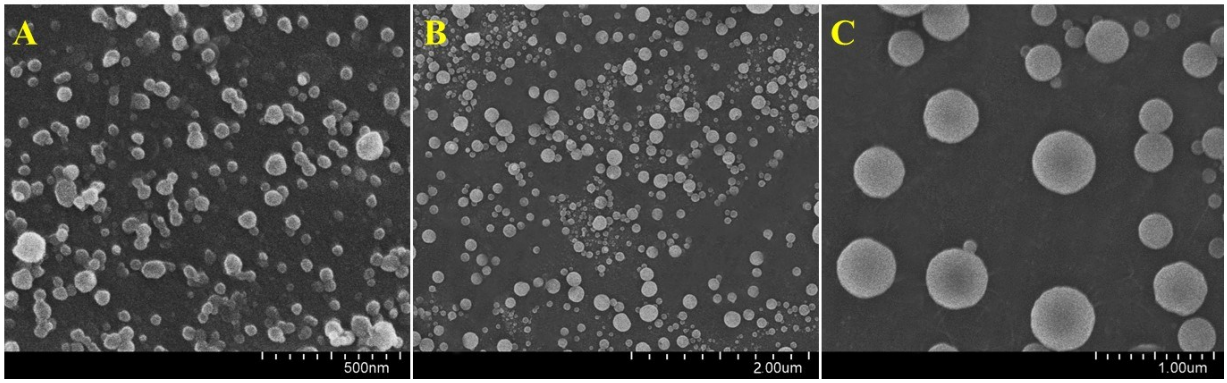

Fig. S5 SEM images of the PC-PNPs synthesized with different concentrations of the PC solution. (A) 5 mg/mL, (B) 20 mg/mL, (C) 40 mg/mL.

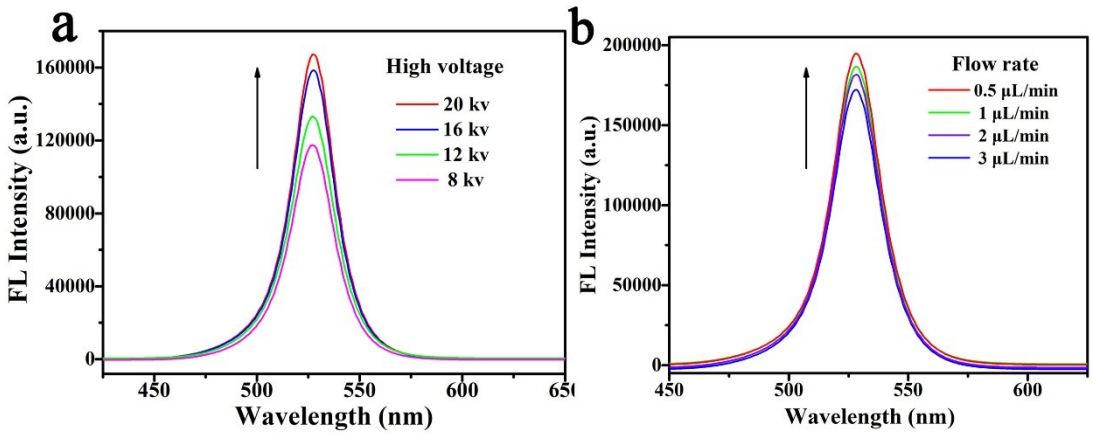

Fig. S6 FL spectra of PC-PNPs prepared with (a) different spraying voltages, 8, 12, 16, 20 kv, respectively; and (b) different flow rates, 3, 2, 1, 0.5 μL/min, respectively.

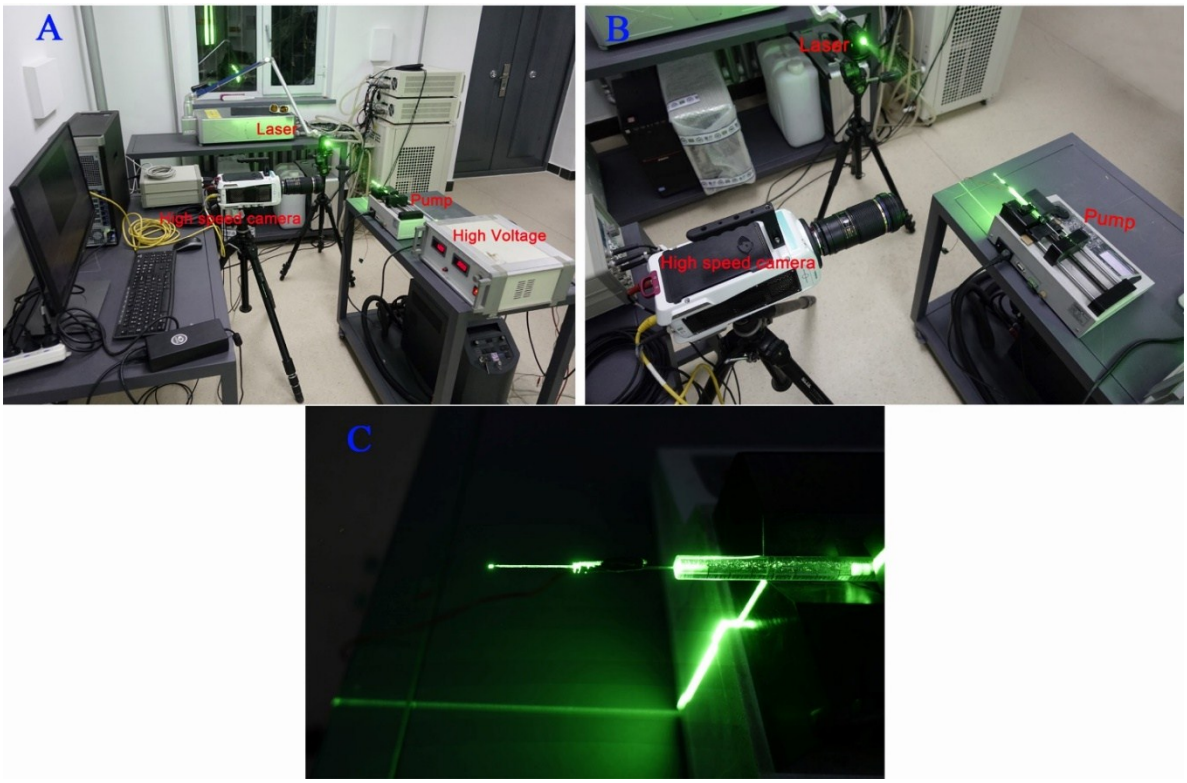

Fig. S7 PIV setup for speed and trajectory imaging of the microdroplets.

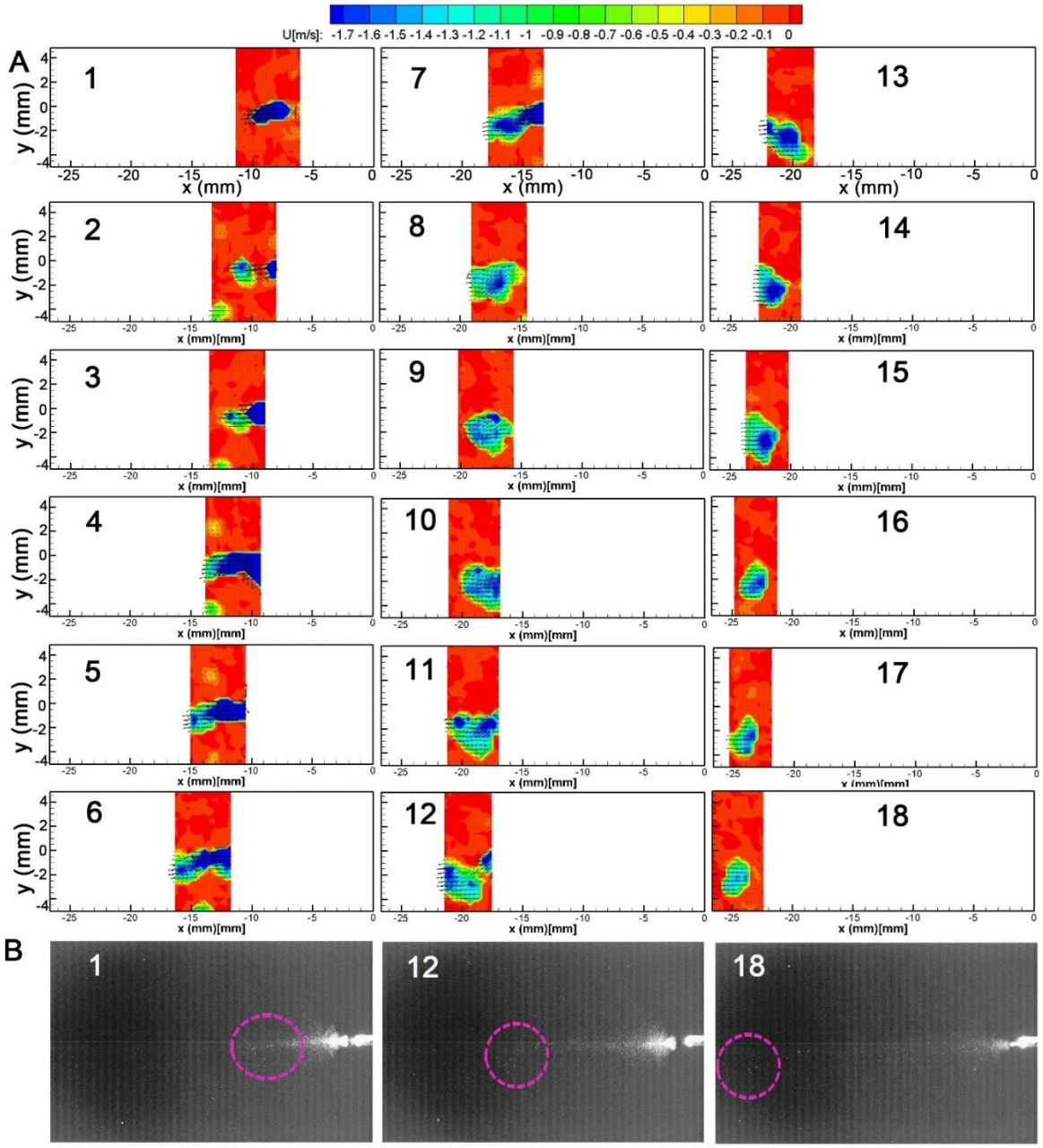

Fig. S8 (A) The average speed of the nanoparticles at different times as measured by PIV. Time gap between each image from 1 to 18 was 0.5 ms. (B) Images of the nanoparticles at different times, corresponds to images 1, 12 and 18 in (A).

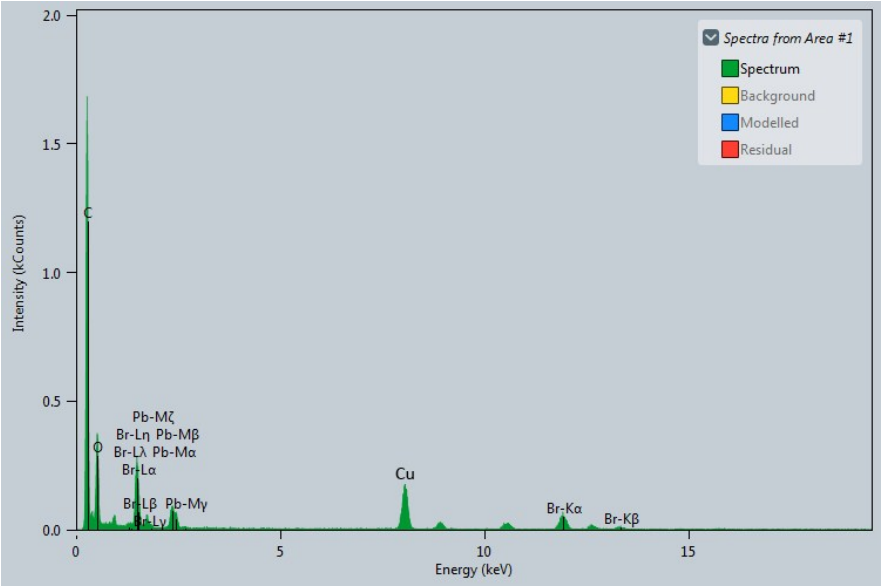

Fig. S9 Energy-dispersive X-ray spectroscopy (EDS) results of the PC-PNPs.

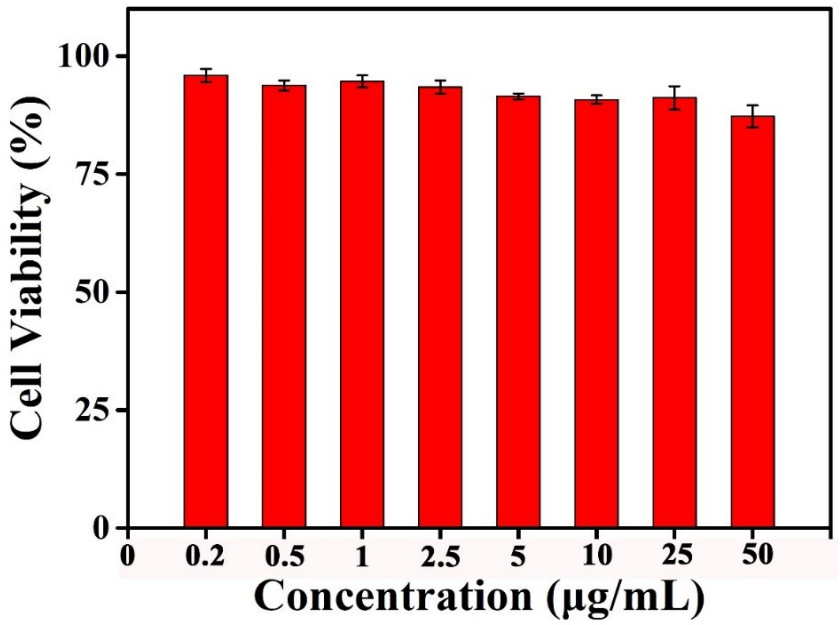

Fig. S10 In vitro cytotoxicity of the PC-PNPs against HepG2 cells at different concentrations after incubation for 24 h.

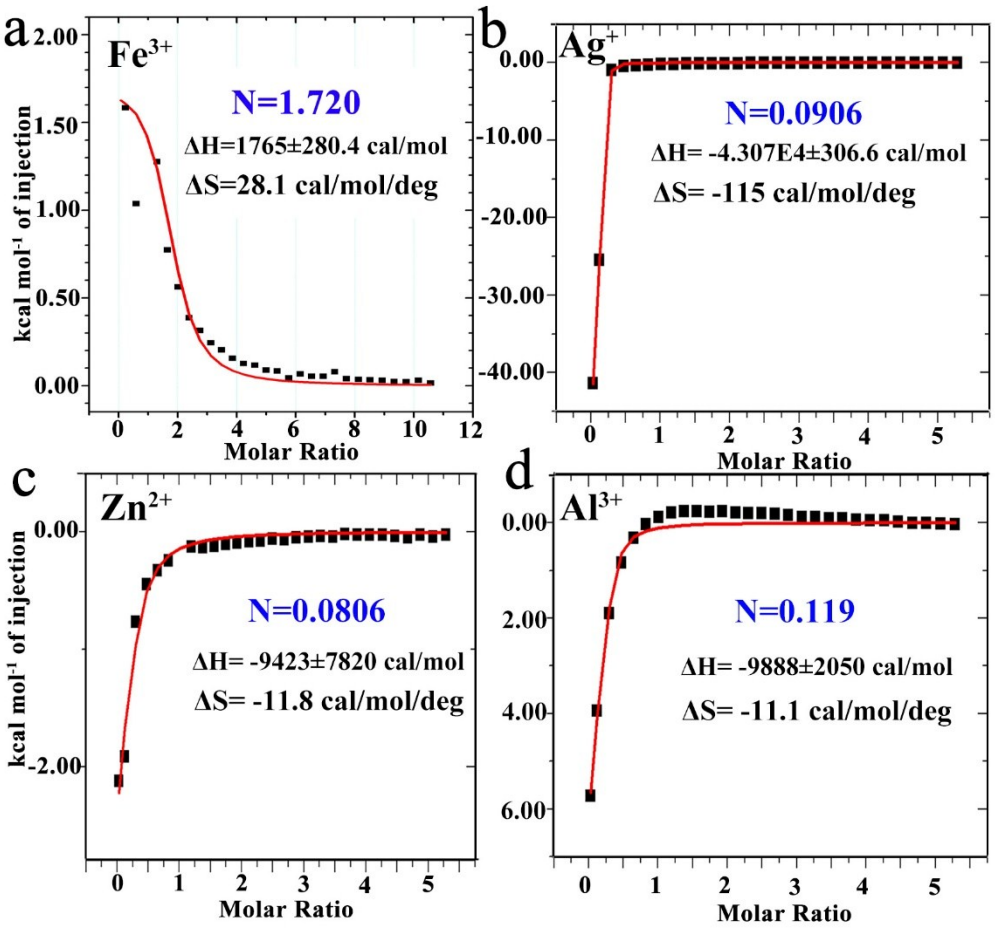

Fig. S11 ITC results of PC-PNPs and different metal ions. (a) Fe^{3+}, (b) Ag^{+}, (c) Zn^{2+}, (d) Al^{3+}.

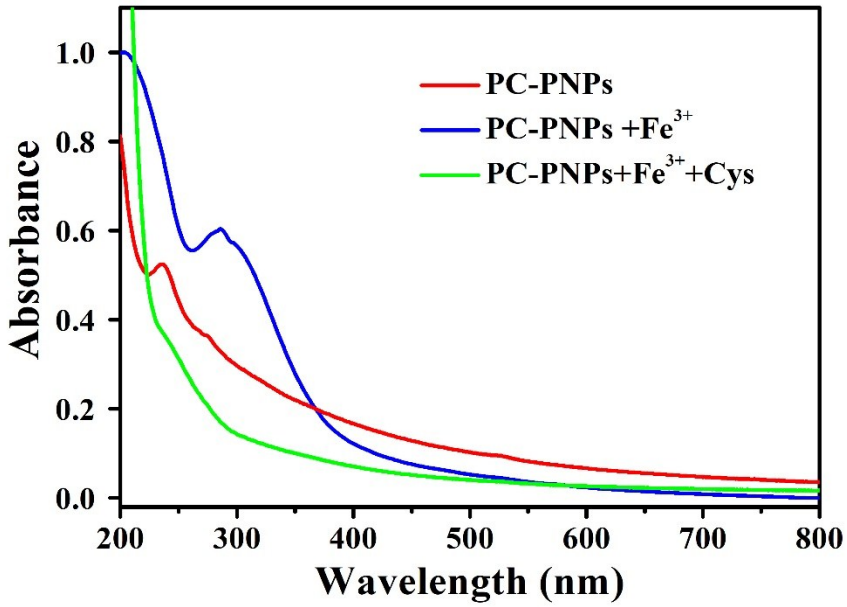

Fig. S12 UV-Vis absorbance of the PC-PNPs (red), PC-PNPs with Fe^{3+} (blue), PC-PNPs with Fe^{3+} and Cys (green).

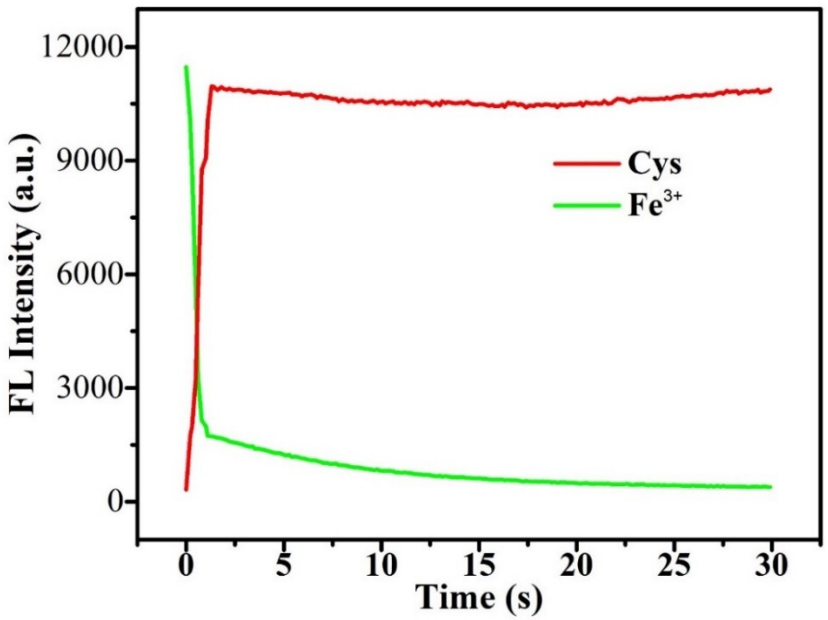

Fig. S13 Time-dependent fluorescence intensity curves of the PC-PNPs upon the addition of Fe^{3+} and then L-Cys.

Reference

(1) Zhang, F.; Zhong, H.; Chen, C.; Wu, X.-g.; Hu, X.; Huang, H.; Han, J.; Zou, B.; Dong, Y. Brightly Luminescent and Color-Tunable Colloidal $CH_3NH_3PbX_3$ (X = Br, I, Cl) Quantum Dots: Potential Alternatives for Display Technology *ACS Nano* **2015**, *9*, 4533-4542.